Separation Science and Technology
Publication details, including instructions for authors and subscription information:
http://www.informaworld.com/smpp/title~content=t713708471

Effects of Operating Conditions on Pressure Drop in a Pulse-Jet Bagfilter for Coke Dust

Jeong-Min Suh[a]; Young-Il Lim[b]; Paul Massarotto[c]; Woo-Taik Lim[d]
[a] Department of Regional Environmental System Engineering, Pusan National University, Samryangjin-eup, Miryang, Kyoungnam, Korea [b] Department of Chemical Engineering, Hankyong National University, Gyonggi-do, Anseong-si, Korea [c] School of Chemical Engineering, University of Queensland, Brisbane, Australia [d] Department of Applied Chemistry, Andong National University, Andong, Kyungpook, Korea

Online publication date: 02 June 2010

To cite this Article Suh, Jeong-Min , Lim, Young-Il , Massarotto, Paul and Lim, Woo-Taik(2010) 'Effects of Operating Conditions on Pressure Drop in a Pulse-Jet Bagfilter for Coke Dust', Separation Science and Technology, 45: 9, 1228 — 1239
To link to this Article: DOI: 10.1080/01496391003775840
URL: http://dx.doi.org/10.1080/01496391003775840

Separation Science and Technology, 45: 1228–1239, 2010

ISSN: 0149-6395 print/1520-5754 online
DOI: 10.1080/01496391003775840

Taylor & Francis
Taylor & Francis Group

Effects of Operating Conditions on Pressure Drop in a Pulse-Jet Bagfilter for Coke Dust

Jeong-Min Suh,[1] Young-Il Lim,[2] Paul Massarotto,[3] and Woo-Taik Lim[4]

[1]*Department of Regional Environmental System Engineering, Pusan National University, Samryangjin-eup, Miryang, Kyoungnam, Korea*
[2]*Department of Chemical Engineering, Hankyong National University, Gyonggi-do, Anseong-si, Korea*
[3]*School of Chemical Engineering, University of Queensland, Brisbane, Australia*
[4]*Department of Applied Chemistry, Andong National University, Andong, Kyungpook, Korea*

A pilot-scale pulse-jet bagfilter was designed, built, and tested for the effects of four operating conditions (filtration velocity, inlet dust concentration, pulse pressure, and pulse interval time) on the total system pressure drop, using coke dust from a steel mill factory. Four models were used to predict the total pressure drop according to the operating conditions. These model parameters were estimated from the 192 experimental data points. The filtration velocity has been determined to be the most relevant variable affecting the pressure drop. An efficient operating condition considering the four variables is proposed from analysis of the dimensionless group model.

Keywords coke dust; dimensional analysis; modeling; operating conditions; pressure drop; pulse-jet bagfilter

INTRODUCTION

The pulse-jet fabric bagfilter is one of the most common items of plant for removing particles from process gases (1,2). The fabric filters are built for the separation of particles from gases with large variation in flowrates from a few cubic meters per hour up to several million cubic meters per hour (3). Dust concentrations in the raw gas may vary from below $1\,g/m^3$ up to several $100\,g/m^3$. These bagfilters can achieve clean gas concentrations below $5\,mg/m^3$ even for submicron particles loading. The dust-collecting performance of bagfilters depends on many factors: the geometry of the baghouse, the fluid flow distribution in the inlet gas, the characteristics of filter media, the gas composition, temperature and pressure, and the particle properties (3). In a bagfilter, particles are transported with the gas to the filter felt where the gas flows through the porous filter medium. During the operation, a cake of dust builds up on the outside of the felt-filter fabric. The growth of this cake increases the pressure drop of the filter and makes periodic cleaning necessary.

The pulse-jet regeneration system enables high separation forces due to the resulting pressure wave moving inside the filter bag. The operation involves injecting high-pressure backpulse air at 3–7 bar into the filter bags for a very short time (50–150 ms) (4). The short burst of compressed air is discharged from a nozzle and usually directed through a venturi into the filter bag to increase the pulse pressure within the bag. The characteristics of the nozzle-venturi system vary with the pulse pressure, nozzle diameter, venturi geometry, and the injection distance between the nozzle and the venturi (5).

The design of the baghouse often depends on the experience of suppliers and users, because the determination of filtration velocity (or baghouse size) has little relevance with the physical models in industrial practice (3). The main operating parameters in the pulse-jet bagfilter are the pressure drop and the filtration velocity. Pressure drop caused by the filter bag and dust cake resistance on the filter is a major contributor to the overall energy consumption (6). The filtration velocity (being gas volume flowrate divided by the total filtering area) determines the unit size and thus the capital cost. The higher filtration velocity means less fabric, therefore less capital cost. However, the higher filtration velocity can lead to the higher pressure drop forcing energy operating costs up (7).

The pressure drop across a bagfilter is influenced by many factors such as the diameter of the injection nozzle and its distance from the bag, pulse pressure, pulse duration, pulse interval time, filtration velocity, inlet dust concentration, and dust particle properties (3–5,7–10). Effects of the design parameters and operating conditions on the pressure drop has been investigated for various dusts such as limestone powder (9,11–14), fly ash (2,5,9,15–18), granite powder (9), alumina powder (4,19),

Received 16 September 2009; accepted 22 February 2010.
Address correspondence to Young-Il Lim, Laboratory Functional Analyses of Complex Systems (FACS), Department of Chemical Engineering, Hankyong National University, Gyonggi-do, Anseong-si Jungang-ro 167, 456-749 Korea. Tel.: +82 31 670 5207; Fax: +82 31 670 5445. E-mail: limyi@hknu.ac.kr

phosphoric rock powder (20), and milk powder (21). Most research has been focused on fine particles under 10 μm (mainly for limestone and fly ash) (4,6,11–15, 18,19,22,23). The mean dust particle diameter ranged between 10 μm and 30 μm in the literatures (17,20). The ceramic filter has been used for hot-gas filtration (17,24,25). For the prediction of the pressure drop as a function of the operating conditions, models have been developed for static (8,9,17,26) and dynamic (24,27) conditions during the operating time or cycle. Recently, the effects of dust cake compaction and thickness on pressure drop have been examined experimentally and theoretically (6,17,20,22,23,28,29). Simulation studies on the cake formation were carried out to quantify the cake thickness, cake porosity, or pressure drop across the filter (30–32).

Limited studies have been reported on coke dust filtration in the literature. In this study, a pilot-scale pulse-jet bagfilter was constructed to investigate the pressure drop under different operating conditions such as filtration velocity, pulse pressure, dust concentration, and pulse interval time, using coke dust with relatively large particle sizes collected from the steel mill industry. This study aims to examine the effects of four operating variables on the total pressure drop. A dimensionless group model (DGM) is developed to predict the total pressure drop, and to identify the relative contribution of the initial pressure drop, dust cake pressure drop, and redeposition to the total system pressure drop.

EXPERIMENTS

Experiments were conducted in a pilot-scale pulse-jet bagfilter composed of a screw dust feeder, four blow tubes with diaphragm valves, a pressure tank, a baghouse compartment of 16 filter bags, a damper, and an exit fan, as shown in Fig. 1 (33,34). The pilot-scale experimental apparatus was designed and tested for investigating the performance of filtration of a coke dust with various operating conditions (i.e., filtration velocity, pulse pressure, dust concentration, and pulse interval time).

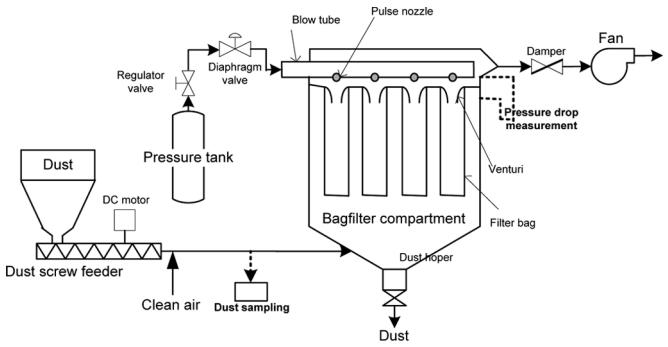

FIG. 1. Schematic diagram of experimental apparatus.

The dust collected in a coke factory of a steel mill industry is supplied through the screw feeder, where the entry dust quantity is regulated by changing the rotation velocity of the screw feeder by means of a 24 V direct current (DC) motor. The concentration of the dust dispersed by clean air varies in the range of $0.5 \sim 3\,g/m^3$. The clean air is aspirated by the suction fan at the exit. Four blow tubes located at the top of the bagfilters are installed with four pulse nozzles per each blow tube oriented to the center of each filter cloth. The compressed air from the air tank is regulated with the pulse pressure of $3 \sim 6\,kg_f/cm^2$. The compressed air is injected for 0.1 s through the pulse nozzle, which is operated by a diaphragm valve for each blow tube. In this study, the pulse nozzle diameter is set to 10 mm. The dust cake on the filter fabric is removed by jet-pulses, where only one row of four blow tubes (i.e., 4 over 16 filter bags) is jet-pulsed at a time with the pulse interval time (Δt) of 30, 50, 70, or 90 s.

A conventional type of venturi is used, as shown in Fig. 2. The injection distance between the nozzle and the venturi is set to 0.11 m, which has previously shown maximum filtration efficiency. The filter cloth is a polyester filter felt without surface coating being used in baghouses of the steel mill industry. There are 16 filter cloths with 0.85 m length and 0.14 m diameter in the rectangular bagfilter compartment. Therefore, the total filtration area is about $6\,m^2$, as shown in Table 1. Table 2 presents the physical properties of the filter felt. The filtration felt used in the steel mill industry is planned to operate for one year. Table 3 reports the characteristics and an ultimate analysis of the coke dust, which contains C, SiO_2, Al_2O_3, CaO, and T-Fe over than 90% in weight. The volumetric mean diameter (VMD) was measured by a Laser particle size analyzer (LS 13320-Dry powder module, Beckman Coulter, USA) to be 58.9 μm, ranging from 0.5 μm to 400 μm.

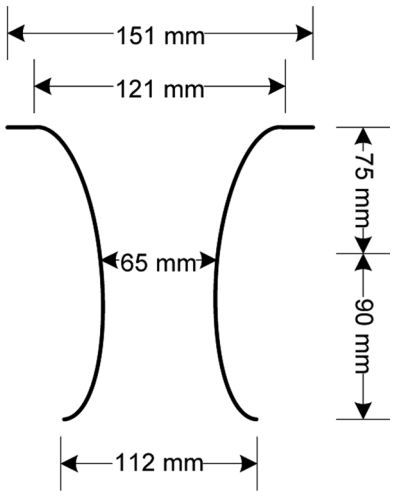

FIG. 2. Venturi geometry used in this study.

TABLE 1
Design specifications and operating conditions

Design specifications			
Bagfilter diameter (D_{bag}, m)	0.14	Pulse nozzle diameter (m)	0.01
Bagfilter length (L_{bag}, m)	0.85	Injection distance (m)	0.11
Total filter area (A_{total}, m^2)	5.98	Venturi throat diameter (D_v, m)	0.065
Number of bags	16		
Operating conditions			
Filtration velocity (v_f, m/min)	1.0, 1.5, 2.0, and 2.5	Pulse interval (Δt, s)	30, 50, 70, and 90
Inlet dust concentration (c_{in}, g/m^3)	0.5, 1.0, 2.0, and 3.0	Pulse duration (s)	0.1
Pulse pressure (P_{pulse}, kPa)	294, 490, and 588	Operating time (t, min)	210

TABLE 2
Characteristics of polyester felt without surface treatment

Specification	Value
Area weight (kg/m^2)	0.564
Felt thickness (mm)	2.34
Breaking strength (kg_f)	169.5
Air permeability ($m^3/m^2/s$)	0.166

The dust was sampled by a Stack Sampler (Model XC-572, Apex Instruments, Inc., USA) after the dust screw feeder (see Fig. 1). The sampled dust was heated and dried for 12 hours at the temperature of 110°C in a conventional oven. The dried dust was cooled down to the room temperature and its weight was measured. The total pressure drop was measured by using a manometer (Dwyer, USA) connected to both the inside and outside of the filter bag in the upper part of the bagfilter compartment, as shown in Fig. 1. The total pressure drop fell instantaneously at the air-pulsing moment and then stabilized within one second. The pressure drop was recorded after stabilization at a given measurement time.

The pressure drop increases linearly after a certain threshold cycle (cycle = $t/\Delta t$, where t is the operating time) and it is sufficient to determine the specific dust cake resistance at an initial stage in pilot-scale testing (26). This threshold cycle was observed at between 30 and 80 cycles (11). In this study, each experiment was carried out for 210 min (i.e., 150–400 cycles). In total, 192 experiments were conducted for four filtration velocities (v_f), four inlet dust concentrations (c_{in}) four pulse interval times (Δt), and three pulse pressures (P_{pulse}). The total pressure drops (ΔP_t^{exp}) across the filter, dust, and venturi were measured.

TABLE 3
Characteristics and ultimate analysis of coke dust

Characteristics						Value
VMD (d_V, μm)						58.9
bulk density of particle (ρ_p, kg/m^3)						801
Ultimate analysis of coke dust (%)						
C	SiO_2	Al_2O_3	CaO	T-Fe	Others	Total
78.60	6.56	2.74	1.45	0.95	9.70	100

MODELING APPROACHES

Four models are presented to predict the bagfilter pressure drop as a function of operating conditions. The first one is the logarithmic multivariate linear regression, where the relative influence of the four operating conditions on the pressure drop is caught. The second model is a classical model used by many researchers (7–9,26). An empirical model (8) is also used to predict the pressure drop. The last one is proposed for the first time in this study, using the dimensionless groups that are related to the total pressure drop expressed by the combination of the initial pressure drop before the dust enters, the dust cake resistance, and the dust redeposition.

Multivariate Linear Regression (MLR)

Multivariate linear regression (MLR) is often used to analyze a data set as a function of the linear combination of individual variables (or operating variables). Logarithmic MLR makes it possible to identify a relative influence of the individual variables on a dependant variable. Logarithmic MLR of the total pressure drop (ΔP_t^{MLR}) is expressed as follows:

$$\Delta P_t^{MLR} = K_0 + K_1 \ln v_f + K_2 \ln c_m + K_3 \ln P_{pulse} + K_4 \ln \Delta t \quad (1)$$

where K_0, K_1, K_2, K_3, and K_4 are the model parameters to be estimated from experimental data. It is worth noting that the slope of ΔP_t^{MLR} versus the logarithm of operating variables

signifies a relative influence with the same dimension. For example, the slope of ΔP_t^{MLR} versus the logarithm of filtration velocity ($\ln v_f$) is:

$$\frac{d\Delta P_t^{MLR}}{d\ln v_f} \equiv \frac{d\Delta P_t^{MLR}}{dv_f/v_f} = K_1 \tag{2}$$

where K_1 has the unit of Pa, which is the same as the others (K_2, K_3, and K_4).

Theoretical Model (TM)

In the theoretical model (TM), the total pressure drop (ΔP_t^{TM}) consists of pressure drops across the fabric (ΔP_f), dust (ΔP_d), and venturi (ΔP_v):

$$\Delta P_t^{TM} = \Delta P_f + \Delta P_d + \Delta P_v \tag{3}$$

Since the first and third terms on the right side of Eq. (3) correspond to the initial pressure drop ($\Delta P_{initial}$) with clean air before the dust enters, Eq. (3) is rewritten:

$$\Delta P_t^{TM} = \Delta P_{initial} + \Delta P_d \tag{4}$$

The initial pressure drop ($\Delta P_{initial}$) with clean air includes all kinds of pressure drops caused by hydrodynamics between the upper and lower parts of the bagfilter compartment where the pressure drop is measured (24). Figure 3 shows the dynamics of the pressure drop typically observed in this experimental study. The total pressure drops were measured at $\Delta t = 90s$ and $c_{in} = 3g/m^3$ for $v_f = 1.5$ *and* $2m/\text{min}$, and $P_{pulse} = 3$, 5, *and* $6kg_f/cm^2$. The $\Delta P_{initial}(t=0)$ tends to converge to a single value, irrespective of pulse pressure, at a given filtration velocity. The initial pressure drop with clean air is obtained from the ordinate intercept of the linear portion of the pressure drop curve at the beginning of the operating time (13).

Two characteristic phases can be distinguished in the total pressure drop with time, as shown in Fig. 3. A rapid increase of the pressure drop at the beginning of time is often referred to as the cake repair (or pore bridging) phase (26). Once a specific threshold time reaches, the pressure drop grows slowly and linearly, which corresponds to the homogeneous deposition phase of the dust cake (26). The pressure drop due to the homogeneous dust cake resistance on the fabric (ΔP_d) is theoretically expressed as a function of filtration velocity (v_f) and areal dust density (w_o) (7–9,20,23,26):

$$\Delta P_d = K_d \; v_f \; w_o \tag{5}$$

The areal density (w_o; g/m^2) of the dust deposit on the bag is defined as:

$$w_o = c_{in} \; v_f \Delta t \tag{6}$$

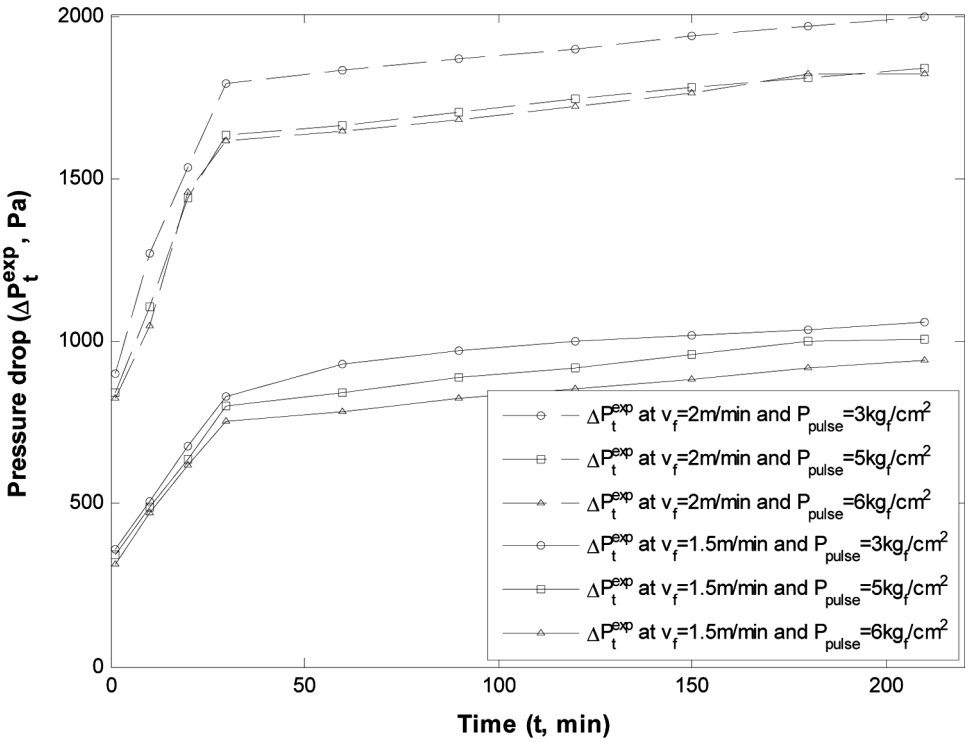

FIG. 3. Total pressure drop versus operating time at $\Delta t = 90\,\text{s}$ and $c_{in} = 3g/m^3$ for different filtration velocities and pulse pressures.

As a result, the theoretical total pressure drop (ΔP_t^{TM}) is obtained as follows, neglecting the effect of the reverse fabric motion (7,9):

$$\Delta P_t^{TM} = \Delta P_{initial}(v_f) + K_d v_f w_o \tag{7}$$

where it is assumed that the initial pressure drop depends only on the filtration velocity (see Fig. 3). $\Delta P_{initial}(v_f)$ and K_d are estimated from the experimental data.

Figure 4 shows the initial pressure drop versus the filtration velocity and Reynolds number for 192 experimental data points. A third-order polynomial equation fits well to this experimental data with a correlation coefficient (R) of 0.999. The empirical equations are shown in Fig. 4 as a function of filtration velocity (v_f) and Reynolds number ($N_{\mathrm{Re}} = \rho_{air} v_f D_{bag}/\mu_{air}$, where $\rho_{air} = 1.2 kg/m^3$ and $\mu_{air} = 1.81 \times 10^{-5} kg/(m \cdot s)$). It is observed that the initial pressure drop increases excessively as the filtration velocity increases. The Reynolds number has a range of $150 < N_{\mathrm{Re}} < 400$ in this study.

In general, the pressure drop across the bagfilter housing is proportional to the square of the gas velocity (7). Since the filter fiber is compressed at high filtration velocities (2) and a highly nonuniform distribution of the velocities exists over the filter area (29), the third-order polynomial equation demonstrates the fact that the initial pressure drop is not proportional to the square of the filtration velocity in the pulse-jet bagfilter.

Empirical Model (EM)

Assuming that the coke dust is an incompressible particle, the empirical model (EM) is expressed as (8):

$$\Delta P_t^{EM} = \Delta P_{initial}(v_f) + K_{emp}\ v_f^a w_o^b P_{pulse}^c \tag{8}$$

where K_{emp} is the dust resistance and there are three exponent parameters (*a, b*, and *c*) for the filtration velocity (v_f), areal density (w_o), and pulse pressure (P_{pulse}), respectively. The empirical model may predict well the pressure drop with the three essential influencing factors and the four model parameters. However, EM has such a limitation that it is not easy to attribute physical meaning to the model parameters estimated from experimental data.

Dimensionless Group Model (DGM)

Imperfect filtrations of dust are often observed with jet-pulse filters. The dust cake is incompletely removed and/or the redeposition of removed dust cake takes place (14,29,35). The changes in cake compaction and thickness affect the filtration performance (6,17,20,22,23,28,30–32). Therefore, dimensional analysis is considered to identify dust cake redeposition, cake compaction, and thickness growth, using the total pressure drop measured experimentally as a representative value.

Figure 5 shows the total pressure drop with time at $v_f = 1.5\, m/min$, $c_{in} = 3\, g/m^3$, $P_{pulse} = 6\, kg_f/cm^2$, and $\Delta t = 90$ s. Instantaneous pressure fall-off at the measuring

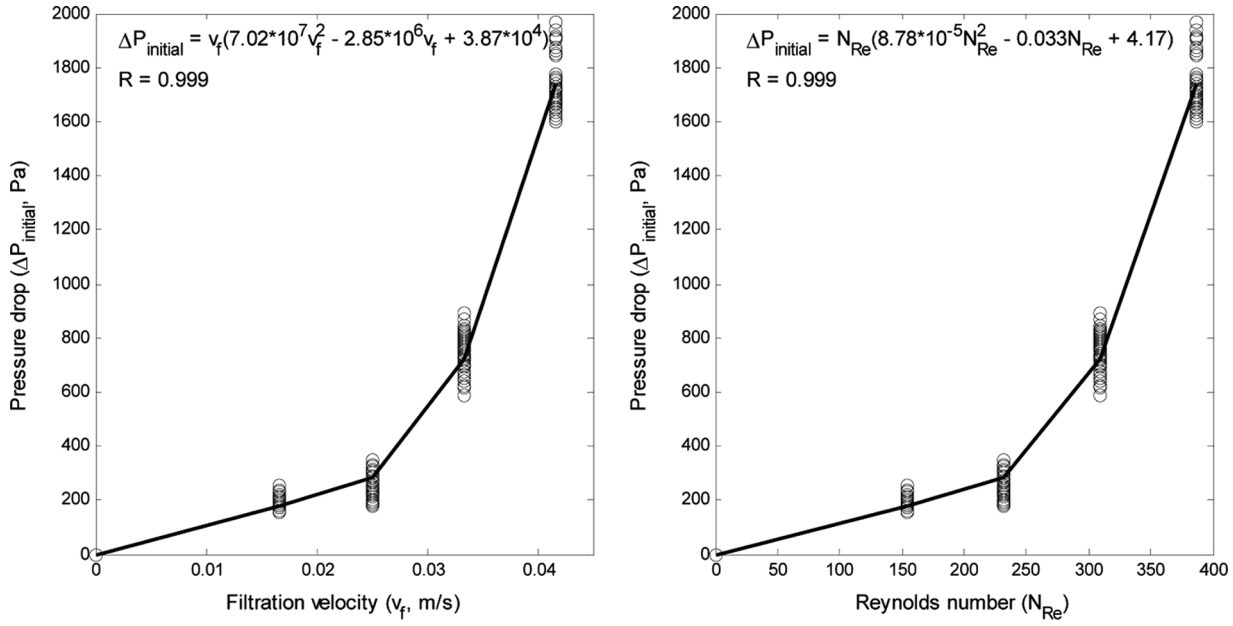

(a) $\Delta P_{initial}(v_f)$ (b) $\Delta P_{initial}(N_{\mathrm{Re}})$

FIG. 4. Initial pressure drop with respect to (a) filtration velocity and (b) Reynolds number.

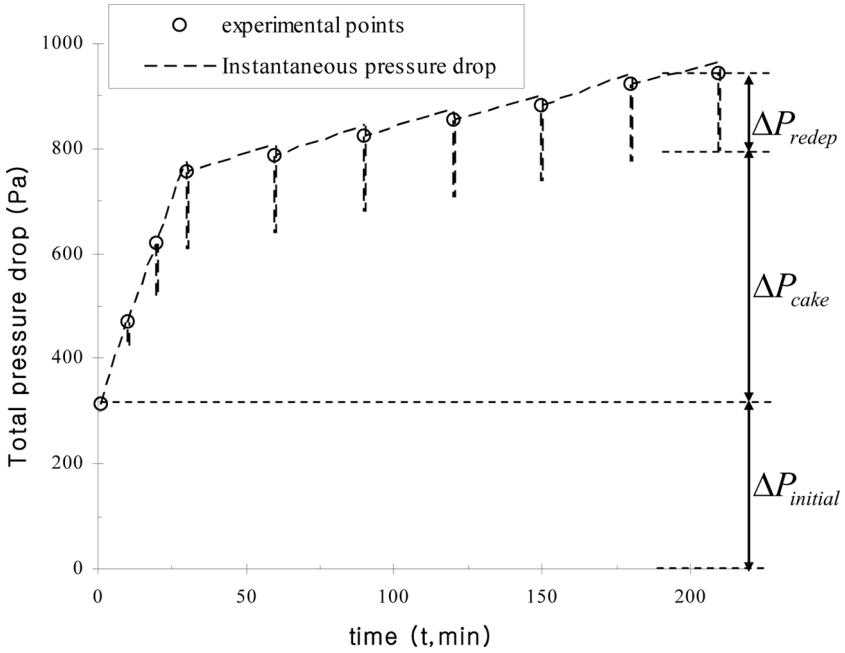

FIG. 5. Experimentally-measured total pressure drop ($\Delta P_t^{\exp}$) divided into three parts: $\Delta P_{initial}$, ΔP_{cake}, and ΔP_{redep}.

time is indicated by the dashed line. The amount of instantaneous pressure fall-off appears constant, during the linear and stable increase in total pressure drop. With the assumption that instantaneous pressure fall-off (ΔP_{redep}) corresponds to prompt redeposition of the dust cake removed by pulse-jet cleaning, the total pressure drop is divided into three portions: initial pressure drop ($\Delta P_{initial}$) at t = 0, cake pressure drop (ΔP_{cake}) caused by unremoval dust cake on the filter, and redeposition pressure drop (ΔP_{redep}) of removed dust cake, as shown in Fig. 5.

$$\Delta P_t = \Delta P_{initial} + \Delta P_{cake} + \Delta P_{redep} \tag{9}$$

The total pressure drop (ΔP_t) of a pulse-jet bagfilter can be described as a function of nine variables for dimensional analysis:

$$\Delta P_t = f(L_{bag}, D_{bag}, v_f, c_{in}, P_{pulse}, \Delta t, \rho_{air}, \mu_{air}, \varepsilon) \tag{10}$$

where L_{bag} and D_{bag} are the filter bag length and diameter, respectively. ρ_{air} is the air density at the room temperature, μ_{air} is the air viscosity, and ε means the porosity of dust cake. v_f, c_{in}, P_{pulse}, *and* Δt are the operating variables. In dimensional analysis, there are several important dimensionless groups such as the Reynolds number ($N_{\mathrm{Re}} = \rho_{air} v_f D_{bag}/\mu_{air}$), the Froude number ($N_{Fr} = c_{\ln} v_f^2/L_{bag}/c_{\ln} g = v_f^2/gL_{bag}$), and the dust thickness number ($N_{thick} = c_{\ln} v_f^2 A/P_{pulse} A = c_{\ln} v_f^2/P_{pulse}$). The Reynolds number ($N_{\mathrm{Re}}$) means the ratio of the inertial force to the viscous force. The Froude number (N_{Fr}) is the ratio of the attraction force by the inlet gas flow to gravity force. N_{Fr} strongly influences the redeposition of the detached dust cake, resulting from the fact that the dust cake detached from the filter bag lies on both the attraction force and the gravity force. The dust cake thickness may depend on a cake adhesion and detaching function. The dust thickness numbers (N_{thick})is defined as the ratio of the dust attraction force to the detaching force by pulsing pressure. Thus, the dust cake thickness is determined by the ratio of the two opposite forces.

The pressure drop across a dust cake with a mean cake porosity (ε) and an average cake thickness (L_{cake}) is expressed by the Ergun equation (6,18), neglecting its second term having much less effect than the first term:

$$\Delta P_{cake} = \frac{150\mu}{d_p^2}\frac{(1-\varepsilon)^2}{\varepsilon^3} v_f L_{cake} \tag{11}$$

By further defining the dust cake compaction number as $N_{comp} = (1-\varepsilon)^2/\varepsilon^3$, the cake pressure drop is expressed by means of the dimensionless group:

$$\Delta P_{cake} = K_c N_{comp}^a N_{thick}^b \tag{12}$$

where K_c is the dust cake resistance, and a and b are the exponents of the compaction number and thickness number, respectively. The mean cake porosity (ε) is related to the areal density (17,23) and is inversely proportional to the filtration velocity (18). It may be approximated as follows:

$$\varepsilon = 1 - \frac{w_o}{\rho_p d_p} \tag{13}$$

where the solidosity ($w_o/\rho_p d_p$) is reasonably assumed to be the ratio of dust cake areal density (w_o) to the particle areal

density ($\rho_p d_p$) (30). Therefore, the compaction number can be rewritten as a function of w_o:

$$N_{comp} = \frac{\rho_p d_p w_o^2}{(\rho_p d_p - w_o)^3} \tag{14}$$

Finally, the dimensionless group method (DGM) to predict the total pressure drop (ΔP_t^{DGM}) is constructed as a function of the dimensionless groups described above:

$$\Delta P_t^{DGM} = \Delta P_{initial}(N_{\mathrm{Re}}) + K_c N_{comp}^a (1 \times 10^{10} N_{thick}{}^b + K_r N_{Fr}^c \tag{15}$$

where the thickness number (N_{thick}) is multiplied by an artificial value (1×10^{10}), to make its value have the same magnitude as that of N_{comp}, for convenience. The artificial value does not affect the exponent value (b) but influences the dust cake resistance (K_c). To investigate the dependency of the experimental total pressure drop on the two dimensionless groups (N_{comp} and N_{thick}), the following logarithmic expression is derived from DGM without the third term:

$$\ln(\Delta P_t^{\exp} - \Delta P_{initial}) \equiv \ln \Delta P_{t,net}^{\exp} = \ln K_c + a \ln N_{comp} + b \ln(1 \times 10^{10} N_{thick}) \tag{16}$$

If the net experimental pressure drop $\Delta P_{t,net}^{\exp}$ has a monotonic relationship with the compaction or thickness number (N_{comp} or N_{thick}), a linear slope of a or b would be obtained when $\ln \Delta P_{t,net}^{\exp}$ is plotted against $\ln N_{comp}$ or $\ln N_{thick}$. Since the slope of the logarithmic plot, the so-called elasticity, is a normalized sensitivity, the bigger elasticity means the stronger influence on the total pressure drop. The dependency of $\ln \Delta P_{t,net}^{\exp}$ on $\ln N_{comp}$ and $\ln N_{thick}$ is shown in Fig. 6 for the 192 experimental data points. The $\ln \Delta P_{t,net}^{\exp}$ term tends to increase with increasing $\ln N_{comp}$ with a correlation coefficient of $\mathrm{R} = 0.725$. This occurs because the areal density (w_o) accumulated on the filter bag surface compresses the dust cake (decreases of ε) and N_{comp} increases. The $\ln N_{thick}$ term shows a stronger linear correlation with $\ln \Delta P_{t,net}^{\exp}$ than $\ln N_{comp}$. Here, N_{thick} influences $\Delta P_{t,net}^{\exp}$ about twice as much as N_{comp}.

DGM has five model parameters (K_c, K_r, a, b, and c) to be estimated from the experimental data. The initial pressure drop ($\Delta P_{initial}$) and redeposition pressure drop (ΔP_{redep}) depend only on the filtration velocity. The dust cake with thickness varying with c_{in}, v_f, and P_{pulse} is treated as a compressible mass according to w_o. In DGM, the three different sources of pressure drop contribute linearly to the total pressure drop.

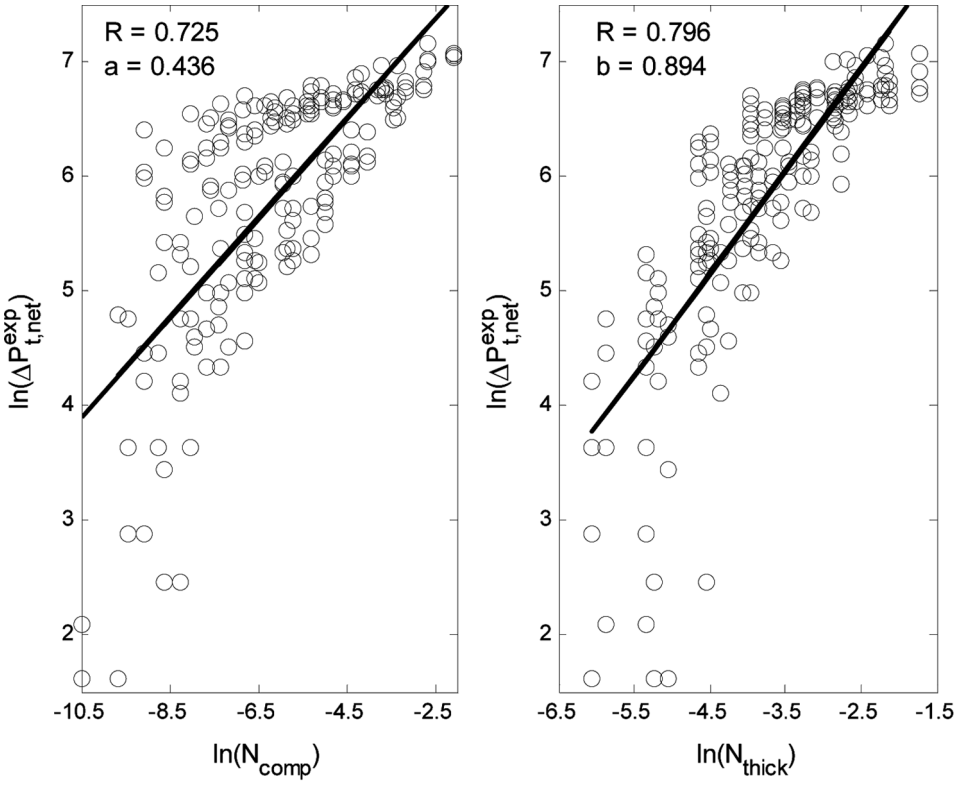

(a) $\ln \Delta P_{t,net}^{\exp}$ with respect to $\ln N_{comp}$ (b) $\ln \Delta P_{t,net}^{\exp}$ with respect to $\ln N_{thick}$

FIG. 6. Dependency of logarithmic net experimental pressure drop on (a) logarithmic compaction number and (b) logarithmic thickness number.

RESULTS AND DISCUSSION

The parameters of the four models presented earlier were estimated from the 192 experimental points, minimizing the mean square error between experimental data and model results. The effects of the operating variables on the pressure drop are analyzed in this section, using the four models and their respective parameters.

Model Comparison

The parameters of the four models are reported in Table 4. The logarithmic MLR reveals that the filtration velocity (v_f) is the most influencing factor on pressure drop. Its effect is about 10 times bigger than that of the other operating variables. The pulse pressure (P_{pulse}) decreases the total pressure drop, as the pulsing pressure detaches the dust cake from the filter bag. The logarithmic MLR shows clearly the relative impact of the four operating variables on the pressure drop, though the correlation coefficient ($R = 0.929$) is slightly lower than the others are.

The theoretical model (TM) often used in the literature is simple and powerful. With only one model parameter (K_d; dust cake resistance) and without considering the pulse pressure (P_{pulse}), TM predicts the total pressure drop well. Since the coke dust particle used in this study is comparatively big, the dust resistance has a small value (see (26) for comparison).

The empirical model (EM) shows the best prediction performance of the four models. However, the empirical model parameters have little physical meaning, as mentioned above. Figure 7 compares the correlation between experimental data and the model predictions of the pressure drop for the four models. The dimensionless group model (DGM) shows a similar behavior as EM in the correlation plot. Four clusters of data points are observed in Fig. 7 (c) and (d): two clusters at the lower part, one cluster in the middle, and one cluster in the upper part. The clustering is mainly associated with the four-filtration velocities.

In Fig. 8, the total pressure drop of the experiment as a function of v_f is compared with that of EM prediction in the four dust concentrations and four pulse interval times at $P_{pulse} = 5\,kg_f/cm^2$. The EM prediction at $P_{pulse} = 5\,kg_f/cm^2$ shows a good agreement with the 64 experimental points over the four filtration velocity (v_f), four dust concentrations (c_{in}), and four pulse intervals (Δt).

Three Sources of Total Pressure Drop

The dimensionless group model (DGM) proposed in this study divides the total pressure drop into three parts: initial pressure drop before the dust enters ($\Delta P_{initial}^{DGM}$), pressure drop by dust cake compressed on the filter bag surface (ΔP_{cake}^{DGM}), and pressure drop by redeposition of dust cake removed from the filter bag (ΔP_{redep}^{DGM}). In Table 4, the five model parameters of DGM are shown. The exponents of N_{comp} and N_{thick} are lowered (see Fig. 6), because the redeposition term is added into the model. The impact of N_{thick} on the total pressure drop is still about twice as much as that of N_{comp}.

Figure 9 depicts the three individual pressure drops at $P_{pulse} = 5\,kg_f/cm^2$ predicted by DGM as a function of v_f at four dust concentrations. Both $\Delta P_{initial}^{DGM}$ (dashed line) and ΔP_{redep}^{DGM} (dot-dashed line) depend only on the filtration velocity (v_f), while ΔP_{cake}^{DGM} (solid lines) varies with all four

TABLE 4
Model parameters estimated from experimental data

Logarithmic multivariate linear regression (MLR)	$\Delta P_t^{MLR} = K_0 + K_1 \ln v_f + K_2 \ln c_{in} + K_3 \ln P_{pulse} + K_4 \ln \Delta t$					
	K_0(Pa)	K_1(Pa)	K_2(Pa)	K_3(Pa)	K_4(Pa)	R
	9.807×10^3	2.264×10^3	0.192×10^3	-0.209×10^3	0.188×10^3	0.929
Theoretical model (TM)	$\Delta P_t^{TM} = \Delta P_{initial}(v_f) + K_d v_f w_o$					
	K_d(Pa · m · s/kg)					R
	3.913×10^3					0.967
Empirical model (EM)	$\Delta P_t^{EM} = \Delta P_{initial}(v_f) + K_{emp} v_f^a w_o^b P_{pulse}^c$					
	K_{emp}	a	b	c		R
	9.318×10^4	1.031	0.360	−0.319		0.988
Dimensionless group model (DGM)	$\Delta P_t^{DGM} = \Delta P_{initial}(N_{Re}) + K_c N_{comp}^a (1 \times 10^{10} N_{thick}^b) + K_r N_{Fr}^c$					
	K_c(Pa)	a	b	K_r(Pa)	c	R
	2.923×10^3	0.162	0.381	6.58×10^4	0.644	0.987

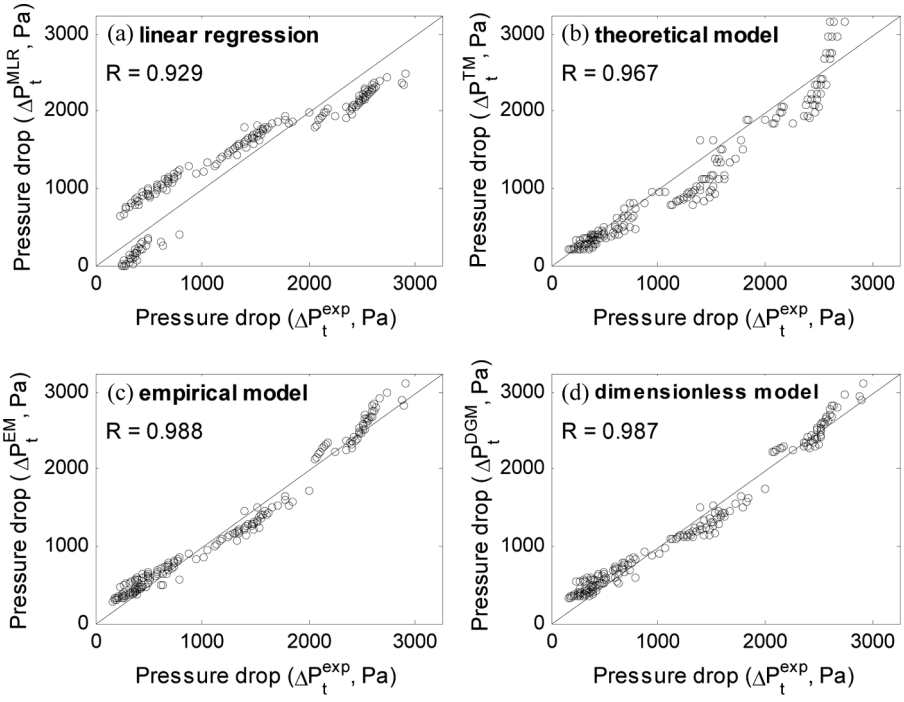

FIG. 7. Correlation plot of pressure drop between experimental data and model predictions.

operating variables (v_f, c_{in}, Δt, and P_{pulse}). ΔP_{redep}^{DGM} ranges from 80 Pa to 280 Pa. Both ΔP_{cake}^{DGM} and ΔP_{redep}^{DGM} tend to increase linearly with the filtration velocity, while $\Delta P_{initial}^{DGM}$ increases exponentially.

$\Delta P_{initial}^{DGM}$ is greater than ΔP_{cake}^{DGM} orΔP_{redep}^{DGM} at $c_m = 0.5$ and $1.0\,g/m^3$ in all the velocities, as shown in Fig. 9 (a) and (b). In these operating conditions, the dust on the filter bag is removed sufficiently by air-jet pulsing, where a longer

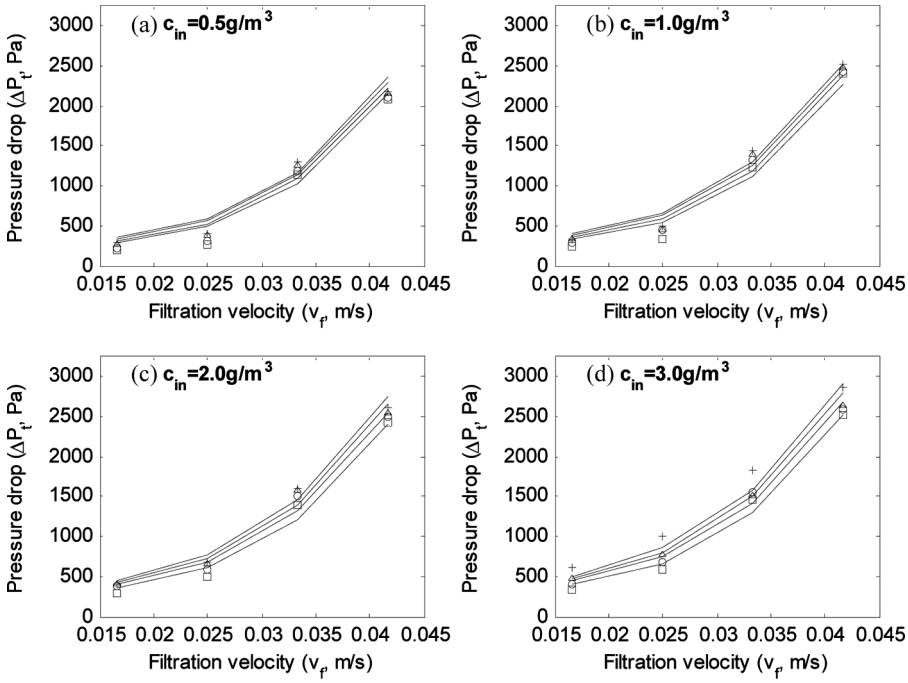

FIG. 8. Comparison of experimental pressure drop (ΔP_t^{exp}) with empirical model (ΔP_t^{EM}) a function of filtration velocity at $P_{pulse} = 5\,kg_f/cm^2$ (□: $\Delta t = 30$ s, ○: $\Delta t = 50$ s, Δ: $\Delta t = 70$ s, +: $\Delta t = 90$ s, and —: model predictions).

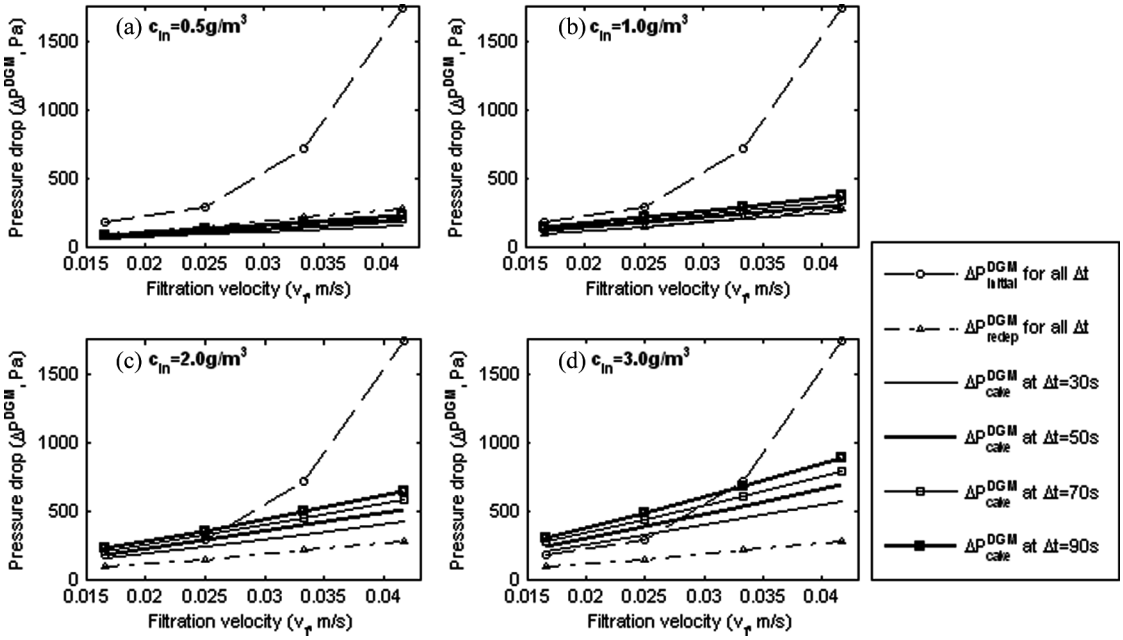

FIG. 9. Pressure drops obtained from DGM (ΔP^{DGM}) as a function of filtration velocity at $P_{pulse} = 5\,kg_f/cm^2$.

pulse interval time than 90 s could be allowed. However, it may not be an efficient operation because of an excessive initial pressure drop greater than 40% of the total pressure drop (see also Fig. 10 (a) and (b)). As the dust concentration increases, ΔP^{DGM}_{cake} rises and becomes a major pressure drop at $c_{in} = 3g/m^3$, as shown in Fig. 9 (d).

The ratios of the three individual pressure drops to the total pressure drop expressed as percentage are shown in Fig. 10. The initial pressure drop (dashed lines) occupies over 50% of the total pressure drop at $c_{in} = 0.5\,g/m^3$. The initial pressure drop at $c_{in} = 1.0\,g/m^3$ still dominates. It is clearly indicated in Fig. 10 that the percentage of the initial

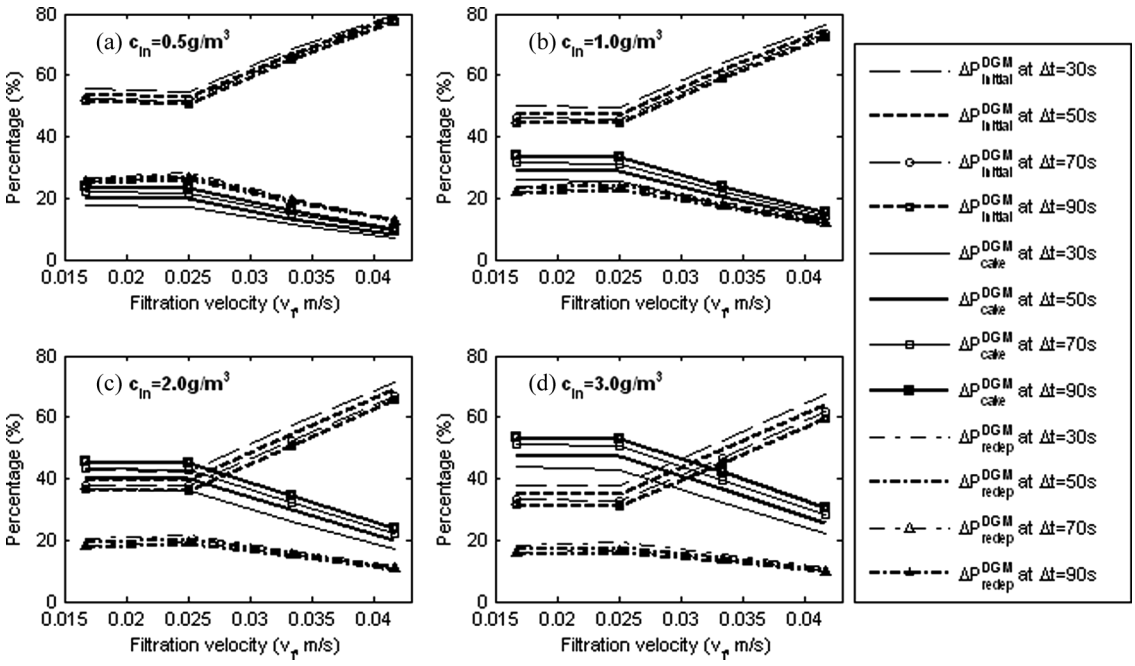

FIG. 10. Percentage of $\Delta P_{initial}, \Delta P^{DGM}_{Redep}$ and ΔP^{DGM}_{cake} to ΔP^{DGM}_{t} as a function of filtration velocity at $P_{pulse} = 5\,kg_f/cm^2$ for four inlet concentrations (c_{in}).

pressure drop increases significantly, when v_f is greater than $0.025\,m/s$. Even though the filtration velocity is preferred to be high at a given filtration area in order to increase the operating capacity, it is better to operate this pulse-jet bagfilter process near $v_f = 0.025\,m/s$ to avoid the extra-charge coming from the high filtration velocity. $\Delta P_{initial}^{DGM}$ (dashed lines) and ΔP_{cake}^{DGM} (solid lines) have similar contribution percentage (about 40%) at $c_{in} = 2\,g/m^3$ and in the low range of filtration velocity, where an efficient operation is expected. At $c_{in} = 3\,g/m^3$, a short pulse interval time (30 s) compared to high pulse times (e.g., 90 s) is better to control the dust cake pressure drop.

CONCLUSIONS

The total pressure drop across a bagfilter is one of the most important factors affecting the operating costs of bagfilter houses. In this study, a pilot-scale pulse-jet bagfilter with about $6\,m^2$ filtration area was designed, built, and tested for the effects of four operating conditions (filtration velocity, inlet dust concentration, pulse pressure, and pulse interval time) on the total pressure drop, using coke dust collected from a steel mill factory.

Four models were applied to predict the total pressure drop according to the operating conditions. These model parameters were estimated from the 192 experimental data points measured at four filtration velocities, four dust concentrations, four pulse interval times, and three pulse pressures. It is demonstrated by the logarithmic multivariate linear regression (MLR) that filtration velocity has about 10 times more effect on the total pressure drop than the three other operating variables. The coke dust cake resistance obtained from the classical theoretical model (TM) is comparatively small because of a large mean particle diameter (about 60 μm). The empirical model (EM) with filtration velocity, areal density, and pulse pressure shows the best correlation coefficient ($R = 0.988$) between experimental data and model predictions.

In this study, the dimensionless group model (DGM) was developed to identify the three main contributors to the total pressure drop: the initial pressure drop, the pressure drop across dust cake, and the redeposition pressure drop. DGM shows essentially the same prediction performance ($R = 0.987$) as EM. The initial and redeposition pressure drops are controlled mainly by the filtration velocity, while the dust cake pressure drop depends on all four operating variables. It is better to operate the pulse-jet bagfilter process near $v_f = 0.025\,m/s$ in order to avoid the overloading coming from high velocities and to maintain high gas-treating capacity. Finally, the ratio of the dust cake pressure drop to the total pressure drop, which is calculated from DGM, can be used as a guideline in finding an efficient operation of the pulse-jet bagfilter.

ACKNOWLEDGEMENTS

Jeong-Min Suh and Young-Il Lim thank The University of Queensland for inviting us as visiting scholars. Special thanks to POSCO (Pohang Steel Company) for supplying the coke dust.

REFERENCES

1. Allen, R.W.K.; Goyder, H.G.D.; Morris, K. (1999) Modelling media movement during cleaning of pulse-jet fabric filters. *Chem. Eng. Res. Des.*, 77 (3): 223.
2. Ellenbecker, M.J.; Leith, D. (1980) The effect of dust retention on pressure drop in a high velocity pulse-jet fabric filter. *Powder Technol.*, 25 (2): 147.
3. Peukert, W.; Wadenpohl, C. (2001) Industrial separation of fine particles with difficult dust properties. *Powder Technol.*, 118 (1–2): 136.
4. Simon, X.; Chazelet, S.; Thomas, D.; Bemer, D.; Regnier, R. (2007) Experimental study of pulse-jet cleaning of bag filters supported by rigid rings. *Powder Technol.*, 172 (2): 67.
5. Tsai, C.J.; Tsai, M.L.; Lu, H.C. (1999) Effect of filtration velocity and filtration pressure drop on the bag-cleaning performance of a pulse-jet baghouse. *Sep. Sci. Technol.*, 35 (2): 211.
6. Chen, Y.S.; Hsiau, S.S. (2009) Cake formation and growth in cake filtration. *Powder Technol.*, 192 (2): 217.
7. Liu, D.H.F.; Liptak, B.G. (1997). Air pollution. In: *Environmental Engineers' Handbook Second Edition*, Lewis Publishers (CRC Press), 346–349.
8. Leith, D.; Ellenbecker, M.J. (1980) Theory for pressure drop in a pulse-jet cleaned fabric filter. *Atmos. Environ.*, 14 (7): 845.
9. Koehler, J.L.; Leith, D. (1983) Model calibration for pressure drop in a pulse-jet cleaned fabric filter. *Atmos. Environ.*, 17 (10): 1909.
10. Hsin-Chung, L.U.; Tsai, C.J. (1996) Numerical and experimental study of cleaning process of a pulse-jet fabric filtration system. *Environ. Sci. Technol.*, 30 (11): 3243.
11. Hindy, K.T.; Sievert, J.; Loeffler, F. (1987) Influence of cloth structure on operational characteristics of pulse-jet cleaned filter bags. *Environ. Int.*, 13 (2): 175.
12. Loeffler, F.; Sievert, J. (1987) Cleaning mechanisms in pulse-jet fabric filters. *Filtr. Sep.*, 24 (2): 110.
13. Tsai, C.J.; Tsai, M.L.; Lu, H.C. (2000) Effect of filtration velocity and filtration pressure drop on the bag-cleaning performance of a pulse-jet baghouse. *Sep. Sci. Technol.*, 35 (2): 211.
14. Saleem, M.; Krammer, G. (2007) Optical in-situ measurement of filter cake height during bag filter plant operation. *Powder Technol.*, 173 (2): 93.
15. Park, S.J.; Choi, H.K.; Park, Y.O.; Son, J.E. (2003) Effects of a shroud tube on flow field and particle behavior inside a bag-filter vessel. *Aerosol Sci. Technol.*, 37 (9): 685.
16. Dean, A.H.; Cushing, K.M. (1988) Survey on the use of pulse-jet fabric filters for coal-fired utility and industrial boilers. *J. Air Pollut. Control Assoc.*, 38 (1): 90.
17. Choi, J.H.; Bak, Y.C.; Jang, H.J.; Kim, J.H. (2004) Experimental investigation into compression properties of integrated coal gasification combined cycle fly ashes on a ceramic filter. *Korean J. Chem. Eng.*, 21 (3): 726.
18. Chen, Y.-S.; Hsiau, S.-S. (2009) Influence of filtration superficial velocity on cake compression and cake formation. *Chem. Eng. Process.*, 48 (5): 988.
19. Calle, S.; Contal, P.; Thomas, D.; Bemer, D.; Leclerc, D. (2002) Evolutions of efficiency and pressure drop of filter media during clogging and cleaning cycles. *Powder Technol.*, 128 (2–3): 213.
20. Silva, C.R.N.; Negrini, V.S.; Aguiar, M.L.; Coury, J.R. (1999) Influence of gas velocity on cake formation and detachment. *Powder Technol.*, 101 (2): 165.

21. Gabites, J.R.; Abrahamson, J.; Winchester, J.A. (2008) Design of baghouses for fines collection in milk powder plants. *Powder Technol.*, 187 (1): 46.
22. Aguiar, M.L.; Coury, J.R. (1996) Cake formation in fabric filtration of gases. *Ind. Eng. Chem. Res.*, 35 (10): 3673.
23. Cheng, Y.H.; Tsai, C.J. (1998) Factors influencing pressure drop through a dust cake during filtration. *Aerosol Sci. Technol.*, 29 (4): 315.
24. Doring, N.; Meyer, J.; Kasper, G. (2009) The influence of cake residence time on the stable operation of a high-temperature gas filter. *Chem. Eng. Sci.*, 64 (10): 2483.
25. Duo, W.; Kirkby, N.F.; Seville, J.P.K.; Clift, R. (1997) Patchy cleaning of rigid gas filters – I. A probabilistic model. *Chem. Eng. Sci.*, 52 (1): 141.
26. Strangert, S. (1978) Predicting performance of bag filters. *Filtr. Sep.*, 15 (1): 42.
27. Ju, J.; Chiu, M.-S.; Tien, C. (2001) Further work on pulse-jet fabric filtration modeling. *Powder Technol.*, 118 (1–2): 79.
28. Stamatakis, K.; Tien, C. (1991) Cake formation and growth in cake filtration. *Chem. Eng. Sci.*, 46 (8): 1917.
29. Kavouras, A.; Krammer, G. (2003) Distributions of age, thickness and gas velocity in the cake of jet pulsed filters-application and validation of a generations filter model. *Chem. Eng. Sci.*, 58 (1): 223.
30. Jeon, K.-J.; Jung, Y.-W. (2004) A simulation study on the compression behavior of dust cakes. *Powder Technol.*, 141 (1–2): 1.
31. Ni, L.A.; Yu, A.B.; Lu, G.Q.; Howes, T. (2006) Simulation of the cake formation and growth in cake filtration. *Miner. Eng.*, 19 (10): 1084.
32. Hoflinger, W.; Stocklmayer, C.; Hackl, A. (1994) Model calculation of the compression behaviour of dust filter cakes. *Filtr. Sep.*, 31 (8): 807.
33. Kim, S.-T. (2004). *A Study on the Pressure Drop Variance of Pulse Interval, Injection Distance in Pulse-Jet Type Bag Filter*; Milyang: Miryang National Univerity.
34. Jang, Y.-D. (2007). *A Study on the Pressure Drop Variance of Inlet Concentration and Face Velocity in Pulse-Jet Type Bag Filter*; Miryang: Miryang National University.
35. Ellenbecker, M.J.; Leith, D. (1983) Dust removal characteristics of fabrics used in pulse-jet filters. *Powder Technol.*, 36 (1): 13.